Vortex Unsteadiness on Slender Bodies at High Incidence

L. E. Ericsson*
Lockheed Missiles & Space Company, Inc., Sunnyvale, California

Existing experimental evidence of vortex unsteadiness on slender bodies at high incidence is examined. It is found that, for the high laminar Reynolds numbers at which the tests have been performed, a likely source of the transient vortex behavior is the transition-promoting effect of freestream turbulence. By considering the similar effects on transition of Reynolds number, freestream turbulence, and surface roughness, the transition-promoting flow phenomenon provides a consistent explanation also for the observed large effects of roll angle on the vortex-induced asymmetric loads. The experimental results of vortex unsteadiness reinforce earlier established evidence of the existing coupling between body motion and asymmetric vortex shedding, raising concern about rigid and elastic response of long slender bodies.

Nomenclature

c = reference length, $c = d$
C_p = $(p - p_\infty)/(\rho_\infty U_\infty^2/2)$
C_Y = $Y/(\rho_\infty {U_\infty}^2/2)S$
c_y = $dC_Y/d(x/c)$
d = maximum diameter
d' = cross-sectional drag, coefficient $c_d = d'/(\rho_\infty U_\infty^2/2)c$
k_s = roughness height
l = total body length
l_N = nose length
M = Mach number
p = static pressure
Re = Reynolds number, $Re = U_\infty d/\nu_\infty$
S = reference area, $S = \pi d^2/4$
U = velocity
x = axial body-fixed coordinate, distance aft of apex
Y = side force
Δz = translatory amplitude
α = angle of attack
Δ = difference or amplitude
ΔC_{p_1} = $C_p(\varphi) - C_p(-\varphi)$
ΔC_p = oscillation amplitude of ΔC_p
ΔP = $C_p(t) - C_p$ mean
θ_c = cone half angle
θ_A = apex half angle
ν = kinematic viscosity of air
ρ = air density
φ = azimuth angle, $\varphi = 0$ at windward meridian

Subscripts

A = apex
AV = asymmetric vortices
B = body
c = cone
max = maximum
n = normal to body axis
N = nose
t = transition
UV = unsteady vortices
∞ = freestream conditions

Presented as Paper 86-0486 at the AIAA 24th Aerospace Sciences Meeting, Reno, NV, Jan. 6-9, 1986; received Feb. 13, 1986; revision received Aug. 1, 1986.

*Senior Consulting Engineer. Fellow AIAA.

Introduction

THE intermittent, unsteady character of asymmetric forebody vortices was observed by Allen and Perkins,[1] who found that the asymmetry changed between its two possible states in an aperiodic manner. Further investigations by Gowen[2] showed that the pressure coefficient difference $\Delta P = C(t) - C_p$ mean on the leeside of ogive- and cone-cylinders ($\varphi = 157$ deg) varied in a random, aperodic manner (Fig. 1), and that the asymmetric vortex geometry changed between its two extreme positions (Fig. 2). That the change occurs very fast is evidenced by the time histories in Fig. 1. Frame 5 at $\alpha = 36$ deg in Fig. 2 has captured the vortex geometry in the transient position between the two alternative asymmetric states. More recent test results[3,4] show similar intermittent, asymmetric vortex characteristics.

Besides presenting a possible forcing function of the buffet type, the unsteadiness of the asymmetric vortices also indicates a certain proneness for the coupling with vehicle motion described in Refs. 5 and 6. A similar concern was expressed by Gowen and Perkins.[7] "It is realized that for full-scale vehicles in flight there exists the possibility of coupling between the shedding of the wake vortices and the movement of the aircraft." It is largely with this concern in mind that an examination is made in the present paper of the existing database for unsteady vortex shedding on slender bodies at high angles of attack.

It should be emphasized that the experimental results to be discussed were all obtained at zero side slip and subcritical (laminar) crossflow conditions.

Discussion

The aperiodic vortex shedding illustrated by Fig. 1 could be expected to occur at the incipient asymmetric flow conditions, i.e., when $\alpha \approx \alpha_{Av}$. According to Fiechter's results,[8] asymmetric vortex shedding will start occurring at body station x when the angle of attack exceeds $(\alpha_{AV})_B = \tan^{-1}(4.2\, d/x)$. On a pointed, slender nose, asymmetric vortex shedding starts when $\alpha > 2\theta_A$, where $\theta_A = \theta_c$ for a conic nose and $\theta_A = \tan^{-1}\{(l_N/d)/[(l_N/d)^2 - 0.25]\}$ for a tangent-ogive nose.[9,10]

Figure 3 shows the differential pressure coefficient ΔC_p, measured by Hunt and Dexter[4] for $\varphi = \pm 75$ deg, at $x/d = 8$ on an $l_N/d = 3$ ogive cylinder. According to Fiechter's results,[8] at $\alpha = 30$ deg asymmetric vortex shedding should have started at $x/d = 7.2$. Thus, the pressure oscillations are for incipient asymmetric flow conditions, and the oscillations occur around $\Delta C_p = 0$. The results obtained in the high turbulence (0.7%) Bristol tunnel (shown in Fig. 3a), are very

similar to those reported earlier for an $l_N/d=2$ ogive cylinder (Fig. 12 in Ref. 3). Decreasing the freestream turbulence from 0.7% to the 0.01% level existing in the RAE tunnel (see Fig. 3b), essentially eliminated the "flipping" of the vortex asymmetry (the intermittent changing between the two extreme asymmetric vortex geometries). The remaining oscillation is that pertaining to the symmetric vortices. The results obtained by Yanta and Wardlaw[11] are instructive in this respect (see Fig. 4). At station $x/d=5.7$, asymmetric

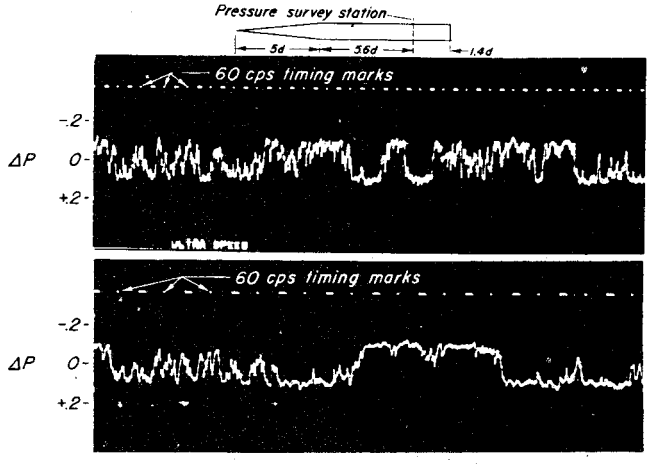

Fig. 1 Pressure variation at $\varphi=157$ deg and $x/d=10.6$ on a cone-cylinder body: $\alpha=23.7$ deg, $M_\infty=1.45$, $Re=0.5\times10^6$ (Ref. 2).

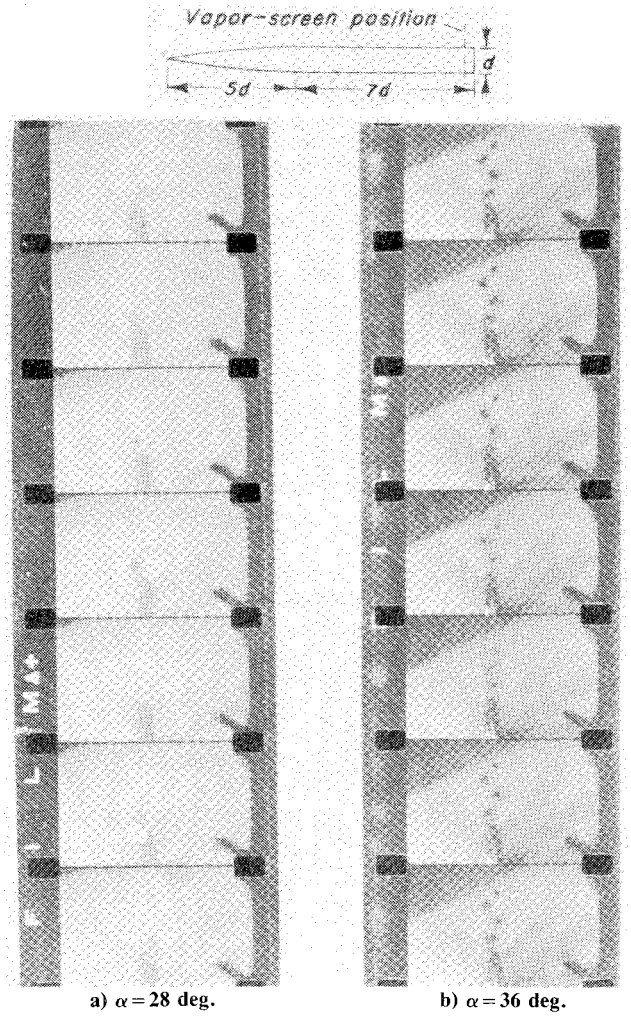

a) $\alpha=28$ deg. b) $\alpha=36$ deg.

Fig. 2 Vapor screen flow pictures of asymmetric vortices on an ogive-cylinder body at $M_\infty=1.98$ and $Re=0.5\times10^6$ (Ref. 2).

vortex shedding should start[8] at $\alpha\approx37$ deg. Thus, it is not surprising that at $\alpha=45$ deg, when the pressures were recorded at two different times, the distribution was symmetric in one case and asymmetric in the other. At $\alpha=45$ deg, asymmetric flow should start at $x/d=4.2$, explaining why symmetric flow conditions were observed at $x/d=2.6$.

When Hunt and Dexter[4] increased the angle of attack to $\alpha=50$ deg, the results shown in Fig. 5 were obtained. The results for the higher turbulence level are somewhat similar to what they were at $\alpha=30$ deg (compare Figs. 3a and 5a), whereas the low-turbulence results now are for asymmetric rather than for symmetric vortices (compare Figs. 3b and 5b). At this angle of attack, the vortex asymmetry starts on the nose, as $(\alpha_{AV})_N=38$ deg for the $l_N/d=3$ pointed ogive. Apparently, $\alpha=50$ deg is close enough to the incipient flow condition to enable the turbulent flow conditions in the Bristol tunnel to cause flipping of the vortex asymmetry, although the bias toward one side is stronger than it was for $\alpha=30$ deg (compare Figs. 3a and 5a). The results obtained at $\alpha=60$ deg for the second asymmetric load cell are similar to those for $\alpha=50$ deg (Fig. 6). The reduced ΔC_p magnitude is to be expected.

As stated by the authors,[4] the results in Figs. 3, 5, and 6 are in basic agreement with the interaction described in Ref. 3 between turbulence-generated freestream vortices and the body vortices. However, the expectation that this vortex interaction also could explain the effect of roll angle on the asymmetric loads was not supported by the test results[4] (Fig. 7). As the effect was present also in the low-turbulence environment, the authors[4] had to conclude that the source was some form of body asymmetry rather than turbulence.

The following simple explanation is an alternative to the somewhat esoteric vortex interaction proposed by Lamont and Hunt.[3] It holds not only for the results in Figs. 3, 5, and 6, but also for those in Fig. 7. The effect of freestream turbulence is simply to cause earlier boundary-layer transition, with associated large effect on the development of asymmetric flow separation.[9,10,12]

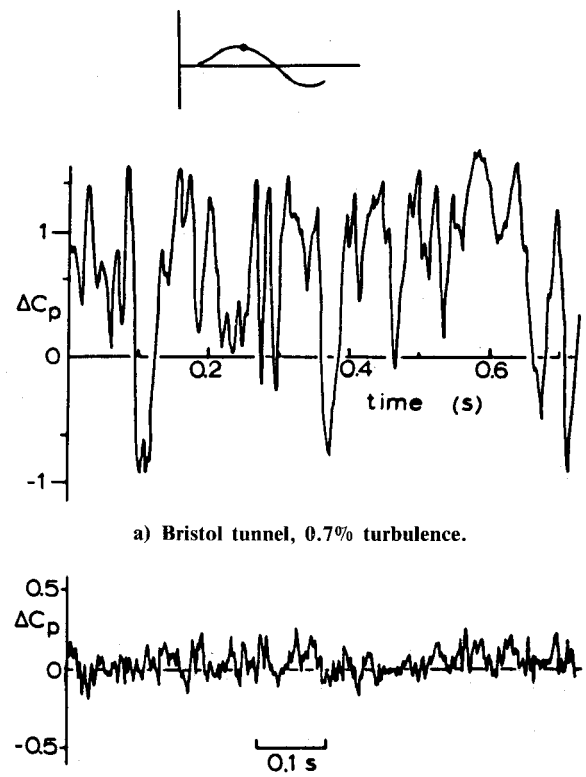

a) Bristol tunnel, 0.7% turbulence.

b) RAE tunnel, 0.01% turbulence.

Fig. 3 Transient pressure difference at $x/d=8$ on an $l_N/d=3$ ogive-cylinder at $\alpha=30$ deg and $Re=0.11\times10^6$ (Ref. 4).

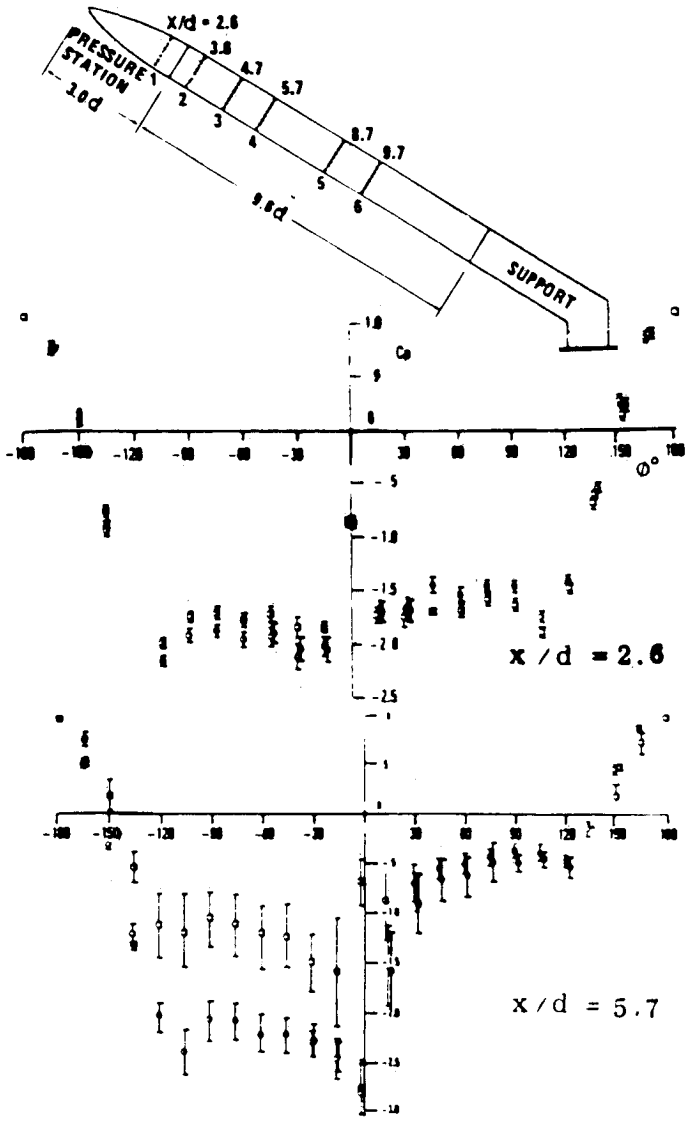

Fig. 4 Pressure distributions at two axial locations on an $l_N/d=3$ ogive-cylinder at $\alpha=45$ deg and $Re=0.11\times10^6$ (Ref. 11).

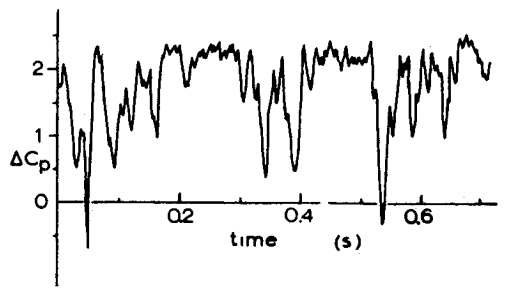

a) Bristol tunnel.

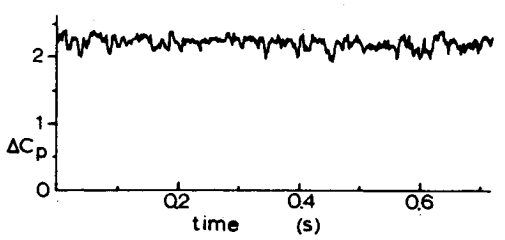

b) RAE tunnel.

Fig. 5 Transient pressure difference on an $\ell_N/d=3$ ogive-cylinder at $\alpha=50$ deg and $Re=0.11\times10^6$ (Ref. 4).

For a circular cylinder normal to the freestream, roughness has been found to have a large effect on the critical Reynolds number and the associated decreased drag[13] (Fig. 8). The variation of drag characteristics observed between different test facilities for a smooth cylinder[14] (Fig. 9), has to be associated with different tunnel turbulence levels. Even when trying to define a roughness Reynolds number for the critical flow region, the results differ by one order of magnitude, depending upon whether they were obtained in the United States or in Europe.[15]

Thus, wind-tunnel turbulence and surface roughness can each change the critical Reynolds number by one order of magnitude. At the high angles of attack where "steady" asymmetric vortices are generated on bodies of revolution, the effective crossflow Reynolds number is $Re=U_\infty d/\nu_\infty$, as has been shown.[9,10,12] The results in Figs. 3-7 were obtained at $Re=10^5$, which would make the crossflow at $\alpha\geq30$ deg subject to boundary-layer tripping through the effects of freestream turbulence and/or surface roughness illustrated in Figs. 8 and 9. The results in Figs. 1 and 2 are for $Re=0.5\times10^6$, still in the range for boundary-layer tripping, especially when considering the effect of Mach number[16] (Fig. 10).

While it is easy to see how the "vortex flipping" can occur at $\alpha\approx\alpha_{AV}$, as in Fig. 3, it is a little more difficult to understand how the same phenomenon can occur at angles of attack far from α_{AV}, as in Figs. 5 and 6. The results[7] in Fig. 11 are illuminating in this respect. For the 4 deg conical

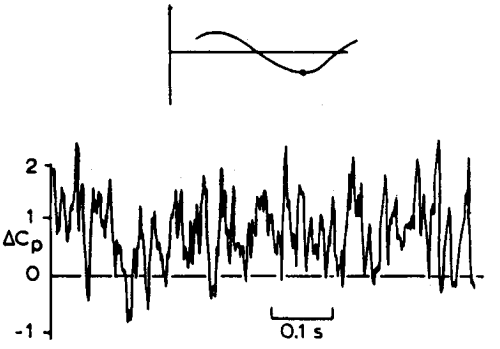

a) Bristol tunnel.

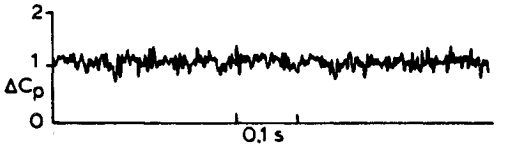

b) RAE tunnel.

Fig. 6 Transient pressure difference at $x/d=5$ on an $l_N/d=3$ ogive-cylinder at $\alpha=60$ deg and $Re=0.11\times10^6$ (Ref. 4).

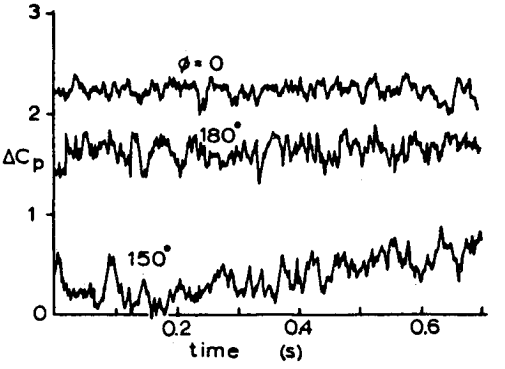

Fig. 7 The effect of roll angle on transient pressure difference at $x/d=4$ on an $l_N/d=3$ ogive-cylinder at $\alpha=50$ deg and $Re=0.10\times10^6$ (Ref. 4).

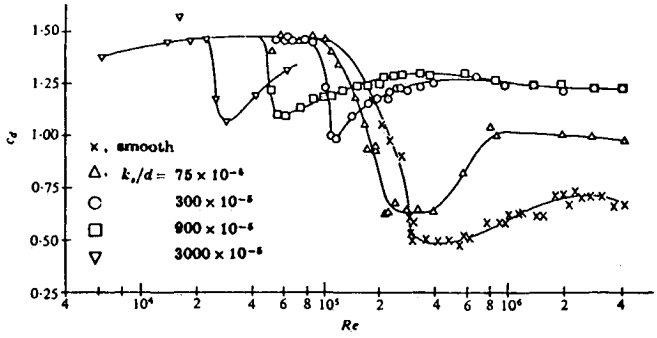

Fig. 8 Effect of roughness on the drag of a circular cylinder (Ref. 13).

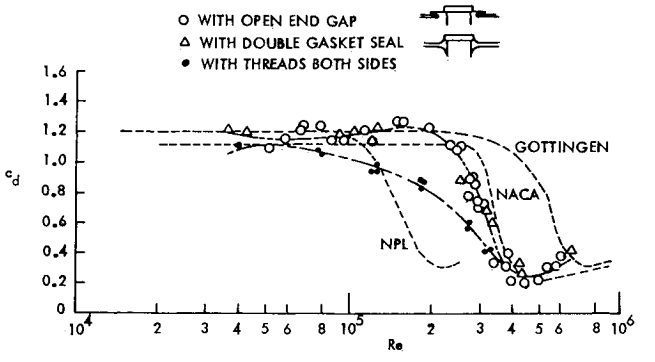

Fig. 9 Cylinder drag coefficient as a function of Reynolds number in different ground facilities (Ref. 14).

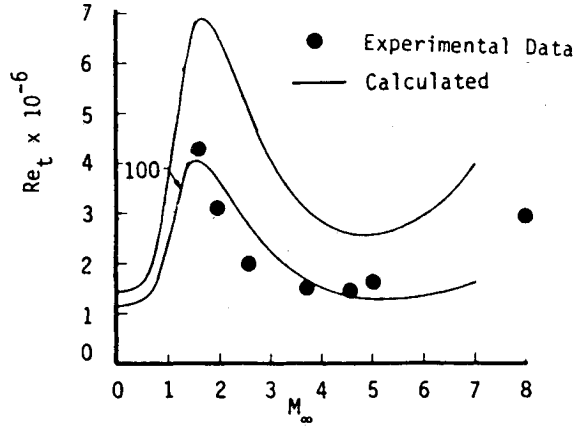

Fig. 10 Effect of Mach number on flat-plate transition Reynolds number (Ref. 16).

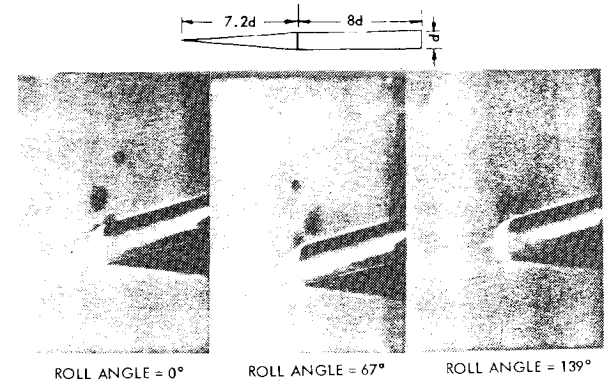

Fig. 11 Effect of roll angle on asymmetric vortex formation on a 4-deg cone-cylinder at $\alpha = 15$ deg, $M_\infty = 2$, and $Re = 0.5 \times 10^6$ (Ref. 7).

nose, $(\alpha_{AV})_N \approx 8$ deg, and for $\alpha = 15$ deg, $\alpha/(\alpha_{AV})_N = 1.875$. In comparison, for the tangent-ogive in Figs. 5 and 6, $(\alpha_{AV})_N \approx 38$ deg, and $\alpha/(\alpha_{AV})_N = 1.31$ and 1.58 for $\alpha = 50$ deg, and 60 deg, respectively. Thus, rolling the ogive-cylinder could potentially bring about the three different vortex geometries shown in Fig. 11. (Note that the crossflow Mach number is well subsonic, $M_n = 0.52$.) Based upon the two-dimensional results shown in Figs. 8 and 9, one can expect that the tripping effects due to asymmetric nose geometry and/or surface roughness (the body microasymmetry) exhibited in Fig. 11 could also be accomplished through nonuniform tunnel turbulence, both effects being similar to that expected for a nonuniform, asymmetric local Reynolds number distribution. Combining this with the Reynolds number effect on "static" asymmetric loads measured by Champigny[17] (Fig. 12), one can see how the high level of freestream turbulence in the Bristol tunnel could generate the large-amplitude unsteadiness shown in Figs. 3, 5, and 6.

Body motion can also influence the boundary layer through the so-called moving-wall effect in a manner equivalent to what would be expected from a nonuniform, asymmetric distribution of the local Reynolds number.[5,6,18] The results for spinning bodies, obtained by Atraghji[19] (Fig. 13) and Kruse[20] (Fig. 14), illustrate how the moving wall effect can compete successfully with the body-fixed microasymmetry even at very low spin rates.

The asymmetric loads measured in static tests are the time-average loads felt by the static balance within its range of frequency response. Lamont and Hunt[3] found this time average to be 30% below the instantaneous asymmetric load in their test. The aperiod, intermittent nature of the unsteadiness can explain the nonrepeatability of static asymmetric loads observed by Oberkampf et al.[21] Hunt and Dexter[4] made sure that the body motion due to sting vibration was negligible in their test. (The amplitude at the nose was below the resolution of the deflection measurements, $\Delta z/d = 0.0004$.) Thus, their results in Figs. 3a, 5a, and 6a are for a stationary model. However, when they increased the angle of attack to $\alpha = 70$ deg, some model motion was observed. This was caused by the unsteady Karman-type vortex shedding occurring on the cylindrical aftbody, as is verified by their unsteady pressure measurements[4] (Fig. 15). The dominant frequency was in good agreement with that expected for Karman vortex shedding, and the oscillation amplitude showed a marked increase at $\alpha > 60$ deg where Karman vortex shedding on the cylindrical aftbody is expected to occur. Thomson observed large C_Y oscillations in the same α range for a cone-cylinder body[22].

At $\alpha = 60$ deg, Lamont and Hunt[3] observed aperiodic pressure oscillations of the type shown in Fig. 1. They were measured one caliber downstream of the $l_N/d = 2$ ogive nose (Fig. 16). Comparing Fig. 16 with Fig. 6a, one is, of course, curious about the difference in unsteady behavior. Following up on the roughness-turbulence equivalence discussed earlier, the experimental results for varying roll angle obtained by Dexter[23] in the low-turbulence (0.01%) RAE tunnel will be examined (Fig. 17). At $\alpha = 50$ deg, the effect of roll angle is so regular that it resembles what one would expect to obtain using a single-nose strake[24] (Fig. 17a). In contrast, when the angle of attack is increased to $\alpha = 65$ deg (Fig. 17b), the load distribution essentially varies between the two mirror states for $|V_y|_{max}$. Why?

The measured effect of freestream Reynolds number on the side force distribution over an ogive-cylinder body[25] (Fig. 18) can be used to illustrate the expected effect of changing the level of uniform freestream turbulence. The figure demonstrates that large freestream fluctuations of the local asymmetric loads (c_y or ΔC_p) can occur simply through fluctuations of the freestream turbulence level, causing the load distribution in Fig. 18 to slide up and down in the axial direction. When considering in addition that the freestream turbulence in ground facilities never is perfectly uniform, one can understand how the experimental results shown in

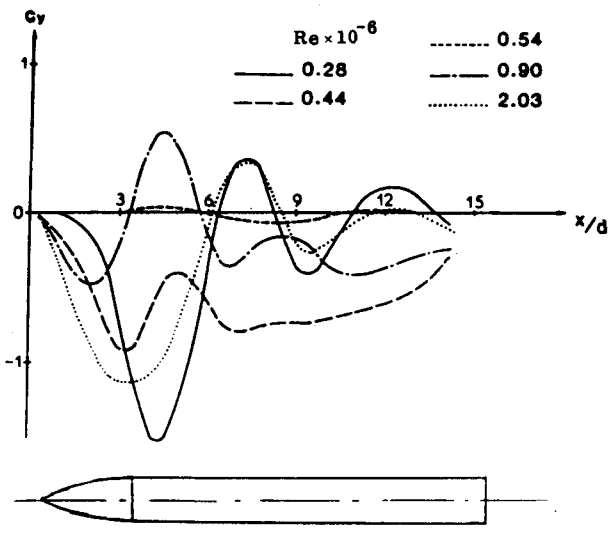

Fig. 12 Side-force distribution on an ogive-cylinder through the critical Reynolds number range at $\alpha = 50$ deg (Ref. 17).

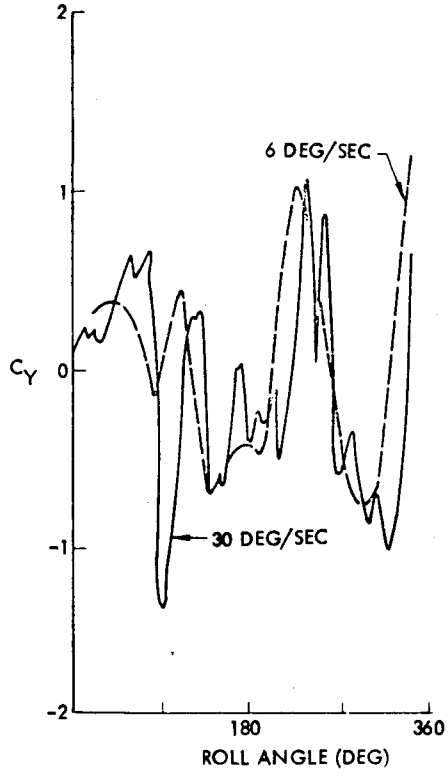

Fig. 13 Effect of roll angle and roll rate on vortex-induced side force of a 5.8 deg cone-cylinder at $\alpha = 18$ deg and $M_\infty = 0.5$ (Ref. 19).

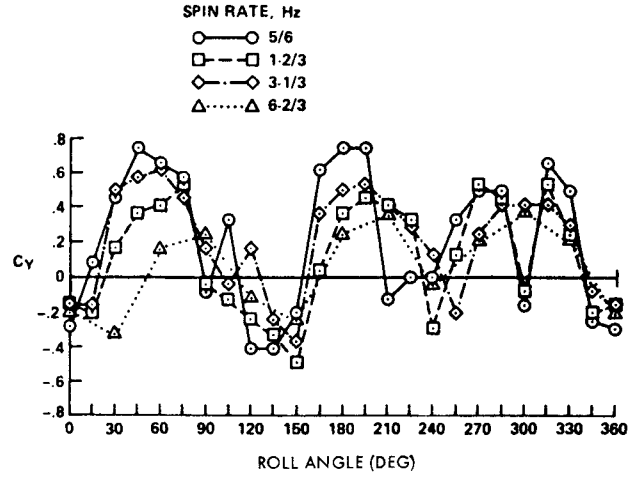

Fig. 14 Effect of spin rate on vortex-induced side force on a 10-deg cone at $\alpha = 58$ deg, $M_\infty = 0.6$ and $Re = 10$ deg (Ref. 20).

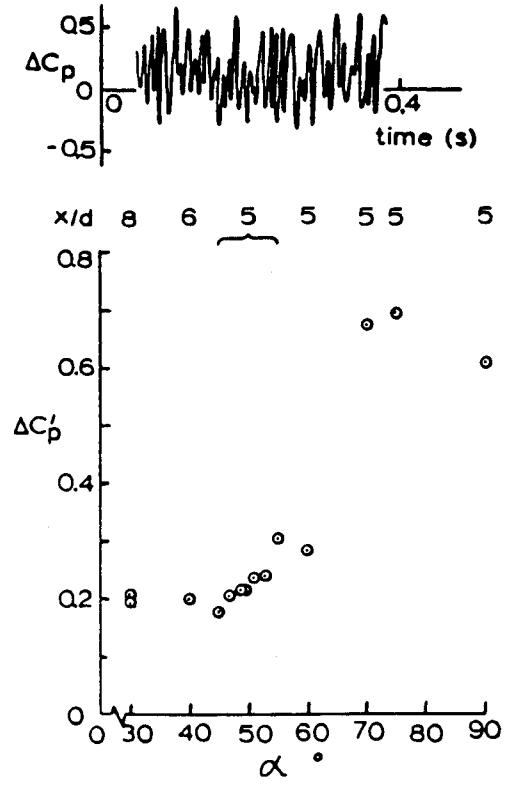

Fig. 15 Increase of fluctuating pressure amplitude when exceeding $\alpha = 60$ deg (Ref. 4).

Figs. 3a, 5a, and 6a can be generated. In regard to the results in Figs. 1 and 16, the following applies:

Considering the roughness/turbulence equivalence, the results in Fig. 18 can also be used to illustrate the effect of nonuniform surface roughness. Rolling the body will pass the roughness asymmetry through the wind-fixed body region where flow separation characteristics are determined. This will cause a variation of the side-force loading similar to that illustrated in Fig. 18, explaining the experimental results in Fig. 17a. In regard to the results in Fig. 17b, they were obtained in the presence of aft-body Karman vortex shedding with associated large disturbance levels (Fig. 15). This presents a disturbance threshold that only very large roughness perturbations can exceed, resulting in the "flip-

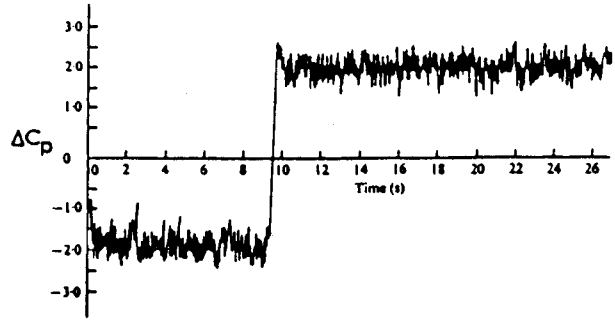

Fig. 16 Aperiodic transient pressure differential at $x/d = 3$ on an $l_N/d = 2$ ogive-cylinder at $\alpha = 60$ deg and $Re = 0.06 \times 10^6$ (Ref. 3).

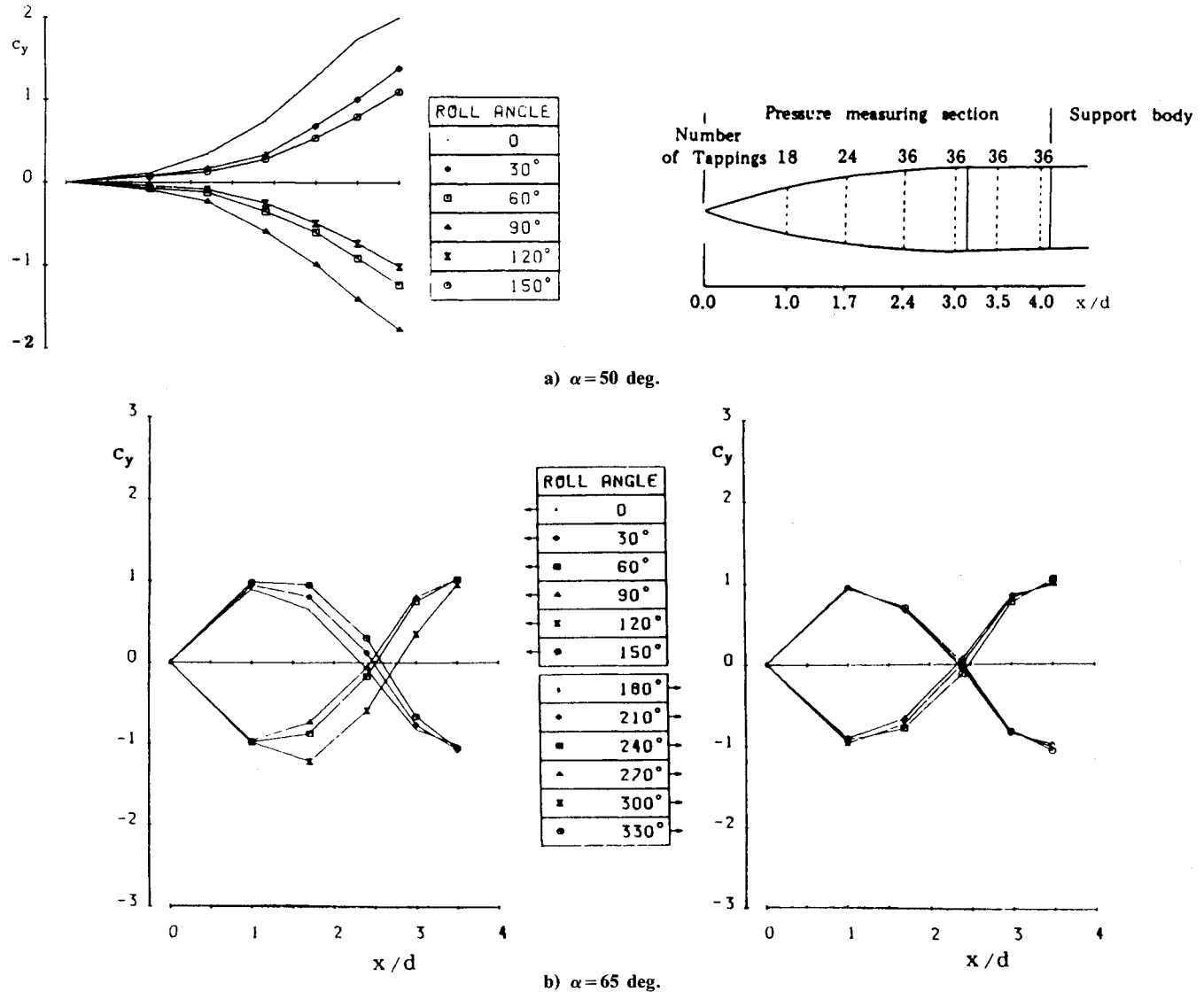

Fig. 17 Effect of roll angle on asymmetric load distribution on ogive-cylinder at $Re = 0.13 \times 10^6$ (Ref. 23).

ping" between alternate vortex asymmetries shown in Fig. 17b. Applying the roughness/turbulence equivalence in the reverse direction, one can see how the results in Figs. 17b and 18 can explain the fluctuating pressure characteristics in Figs. 1 and 16.

Full-Scale Application

Analysis of the experimental evidence of existing basic unsteadiness in the asymmetric vortex shedding from slender bodies at high incidence reinforces the concern expressed by Gowen and Perkins[7] in the early fifties and by the present author and his coauthor at a much later date,[6] i.e., the existence of a strong coupling between the vehicle motion and the asymmetric vortex shedding. So far, only the rigid-body response has been considered. The observed moving wall effects indicate that in free flight the critical flow condition, resulting in the single asymmetric load cell illustrated by the results for $Re = 0.44 \times 10^6$ in Fig. 12, could exist over a range of Reynolds numbers for a maneuvering missile. This would result in the maximum loads described in Refs. 9, 10, and 12. Looking at Fig. 18 and considering that also the moving wall effects[5,6,18] can cause the load distribution to slide axially, one has to be concerned about the elastic vehicle response. In addition to the forcing function of the buffet type that the vortex-unsteadiness generates, there is a potential for negative aerodynamic damping. The latter could be expected to be the more dangerous effect, judging by the flow separation effects observed at lower angles of attack.[26,27]

The always-present problem of scaling becomes especially difficult in regard to the vehicle response to asymmetric vortex shedding. As was stated in the beginning, all the examined experimental results are for subcritical crossflow conditions on the cylindrical aftbody. According to the flow mechanisms postulated in the present paper, the observed vortex unsteadiness resulted because, at the subcritical flow conditions, freestream turbulence, surface roughness, and moving wall effects could promote boundary-layer transition to occur at Reynolds number one order of magnitude below the maximum transition value. Consequently, at the high Reynolds numbers existing in full-scale flight, the problem should disappear. This would be true only for the cylindrical aft body. There will always be a region on the slender nose where boundary-layer transition can be influenced, and judging by the results in Figs. 12 and 18, one can expect significant unsteady vortex-induced loads also at full scale Reynolds numbers. If the vortex-asymmetry were generated by the hydrodynamic instability mechanism proposed by Keener and Chapman,[28] the side-force development on the slender nose should be relatively insensitive to Reynolds

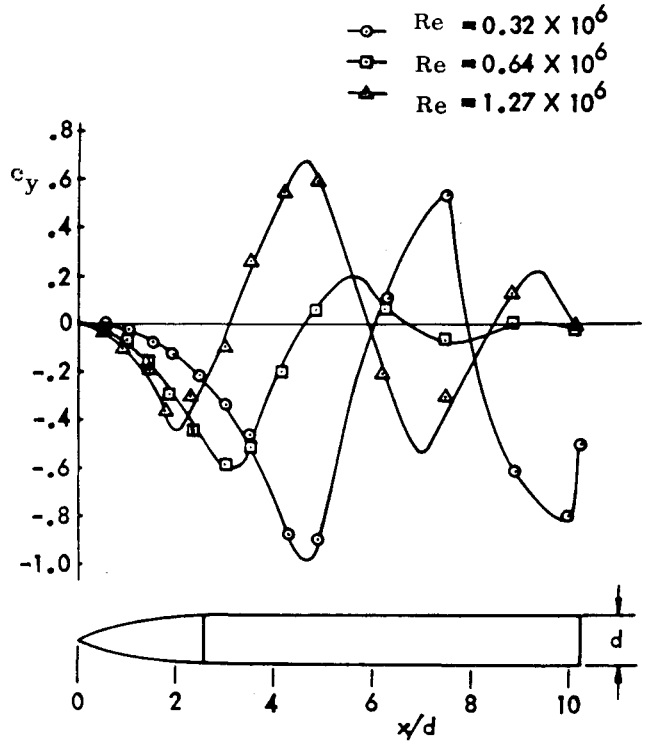

Fig. 18 Side-force distribution as a function of Reynolds number on an ogive-cylinder at $M_\infty = 0.4$ and $\alpha = 50$ deg (Ref. 25).

number. The fact that the experimental results in Figs. 12 and 18 show significant side loads on the nose only for Reynolds numbers high enough to cause transition to occur on the nose leads one to suspect that the vortex unsteadiness observed at subcritical flow conditions will be present also at the supercritical and transcritical flow conditions existing in full scale. Hopefully, the planned tests of an ogive-cylinder body in the National Transonic Facility at NASA Langley Research Center[29] will give us the needed answers in regard to the asymmetric vortex characteristics at very high Reynolds numbers.

Concluding Remarks

An examination of the experimentally documented vortex unsteadiness on slender bodies at high incidence reveals the following.

All the experimental results showing vortex unsteadiness that the author is aware of have been obtained for flow conditions in the upper laminar Reynolds number region. Thus, one likely source of the observed vortex excursions between alternative asymmetric states is the transition-promoting effect of the tunnel turbulence. Between the angle of attack for incipient vortex asymmetry, $\alpha = \alpha_{AV}$, and the one at which Karman vortex shedding occurs on the cylindrical aftbody $\alpha = \alpha_{UV}$, apparently the vortices can also be symmetric for brief instances. However, at $\alpha / \geq \alpha_{UV}$, only the two fully asymmetric vortex geometries can exist, and the switching between them occurs in an aperiodic manner.

When considering the similarity in the effects on transition of Reynolds number, freestream turbulence, and surface roughness, the transition-promoting flow phenomenon provides a consistent explanation also for the observed large effects of roll angle on the vortex-induced asymmetric loads.

In full-scale flight, transition will in general occur on the slender nose. Tests are needed to determine the magnitude of the turbulence-induced transition effects on the asymmetric vortices at full scale Reynolds numbers.

The experimentally documented vortex unsteadiness reinforces earlier expressed concerns about the existing coupling between body motion and asymmetric vortex shedding. In addition to the rigid body dynamics, one also has to be concerned about the elastic response of long slender bodies.

References

[1]Allen, H.J. and Perkins, E.W., "Characteristics of Flow Over Inclined Bodies of Revolution," NACA RMA50L07, March 1951.

[2]Gowen, F.E., "Buffeting of a Vertical Tail on an Inclined Body at Supersonic Mach Numbers," NACA RMA53A09, March 1953.

[3]Lamont, P.J. and Hunt, B.L., "Pressure and Force Distributions on a Sharp-Nosed Circular Cylinder at Large Angles of Inclination to a Uniform Stream," *Journal of Fluid Mechanics,* Vol. 76, Part 3, 1976, pp. 519-559.

[4]Hunt, B.L. and Dexter, P.C., "Pressures on a Slender Body at High Angle of Attack in a Very Low Turbulence Level Air Stream," Paper 17, AGARD CP-247, Jan. 1979.

[5]Ericsson, L.E. and Reding, J.P., "Steady and Unsteady Vortex-Induced Asymmetric Loads on Slender Vehicles," *Journal of Spacecraft and Rockets,* Vol. 18, No. 2, March-April 1981, pp. 97-109.

[6]Ericsson, L.E. and Reding, J.P., "Dynamics of Forebody Flow Separation and Associated Vortices," *Journal of Aircraft,* Vol. 22, No. 4, April 1985, pp. 329-335.

[7]Gowen, F.E. and Perkins, E.W., "A Study of the Effects of Body Shape on the Vortex Wakes of Inclined Bodies at a Mach Number of 2," NACA RM A53I17, Dec. 1, 1953.

[8]Fiechter, M., "Kegelpendelung, Autorotation und Wirbelsysteme Schlanker Flugkörper," *Z. Flugwiss.,* Vol. 20, No. 8, Aug. 1972, pp. 281-292.

[9]Ericsson, L.E. and Reding, J.P., "Review of Vortex-Induced Asymmetric Loads—Part I," *Z. Flugwiss. Weltraumforsch,* Vol. 5, 1981, Heft 3, pp. 162-174.

[10]Ericsson, L.E. and Reding, J.P., "Review of Vortex-Induced Asymmetric Loads—Part II," *Z. Flugwiss. Weltraumforsch.,* Vol. 5, 1981, Heft 6, pp. 349-366.

[11]Yanta W. and Wardlaw, A., "Multi-Stable Vortex Patterns on Slender, Circular Bodies at High Incidence," AIAA Paper 81-0006, Jan. 1981.

[12]Ericsson, L.E. and Reding, J.P., "Aerodynamic Effects of Asymmetric Vortex Shedding from Slender Bodies," AIAA Paper 85-1797-CP, Aug. 1985.

[13]Achenbach, E. and Heinecke, E., "On Vortex Shedding from Smooth and Rough Cylinders in the Range of Reynolds Numbers 6×10^3 to 5×10^6," *Journal of Fluid Mechanics,* Vol. 109, 1981, pp. 239-251.

[14]Humphreys, J.S., "On a Circular Cylinder in a Steady Wind at Transition Reynolds Numbers," *Journal of Fluid Mechanics,* Vol. 9, Part 4, 1960, pp. 603-612.

[15]James, W.D., Paris, S.W., and Malcolm, G.N., "Study of Viscous Crossflow Effects on Circular Cylinders at High Reynolds Numbers," *AIAA Journal,* Vol. 18, No. 9, Sept. 1980, pp. 1066-1072.

[16]Mack, L.M., "Linear Stability Theory and the Problem of Supersonic Boundary Layer Transition," *AIAA Journal,* Vol. 13, No. 3, March 1975, pp. 278-289.

[17]Champigny, P., "Reynolds Number Effect on the Aerodynamic Characteristics of an Ogive-Cylinder at High Angles of Attack," AIAA Paper 84-2176, Aug. 1984.

[18]Ericsson, L.E., "Karman Vortex Shedding and the Effect of Body Motion," *AIAA Journal,* Vol. 18, No. 8, Aug. 1980, pp. 935-944.

[19]Atraghji, E.G., "The Influence of Mach Number, Semi-Nose Angle and Roll Rate on the Development of the Forces and Moments over a Series of Long Slender Bodies of Revolution at Incidence," NAE Data Report 5×5/0020, 1967, National Research Council, Ottawa, Canada.

[20]Kruse, R.L., "Influence of Spin Rate on Side Force of an Axisymmetric Body," *AIAA Journal,* Vol. 16, No. 4, April 1978, pp. 415-416.

[21]Oberkampf, W.L., Owen, F.K., and Shivanda, T.P., "Experimental Investigation of the Asymmetric Body Vortex Wake," AIAA Paper 80-0174, Jan. 1980.

[22]Thomson, K.D., "Estimation at Subsonic Speeds of the Longitudinal and Lateral Aerodynamic Characteristics of Wing-Body Combinations at Angles of Attack up to 90°," Weapons Research Establishment, Salisbury, Australia, Sept. 1976.

[23]Dexter, P.C., "Final Report on an Analysis of the Data Obtained From Low Speed Wind Tunnel Tests of a Three Calibre Tangent Ogive Nose and Cylinder Combination at High Angles of

Incidence," BT 15034, July 1983, Bristol Aerospace, Dynamics Group.

[24]Ericsson, L.E. and Reding, J.P., "Alleviation of Vortex-Induced Asymmetric Loads," *Journal of Spacecraft and Rockets,* Vol. 17, No. 6, Nov.-Dec. 1980, pp. 548-553.

[25]Dahlem, V., Flaherty, J., Sherida, D.E., Pozirembel, C.E.G., "High Angle of Attack Missile Aerodynamics at Mach Numbers 0.3 to 1.5," AFWAL TR-80-3070, Nov. 1980.

[26]Ericsson, L.E. and Reding, J.P., "Analysis of Flow Separation Effects on the Dynamics of a Large Space Booster," *Journal of Spacecraft and Rockets,* Vol. 2, No. 4, July-Aug. 1965, pp. 481-490.

[27]Ericsson, L.E., Reding, J.P., and Guenther, R.A., "Elastic Launch Vehicle Response to Sinousoidal Gusts," *Journal of Spacecraft and Rockets,* Vol. 10, No. 4, April 1973, pp. 244-252.

[28]Keener, E.R. and Chapman, G.T., "Similarity in Vortex Asymmetries over Slender Bodies and Wings," *AIAA Journal,* Vol. 15, No. 9, Sept. 1977, pp. 1370-1372.

[29]Hall, R.M., private communication, Oct. 1985.